

Near-field optical microscopy in liquids

Hiroshi Muramatsu,^{a)} Norio Chiba, Katsunori Homma, Kunio Nakajima,
and Tatsuaki Ataka

Research Laboratory for Advanced Technology, Seiko Instruments Inc., Takatsuka-shinden, Matsudo-shi,
Chiba 271, Japan

Satoko Ohta and Akihiro Kusumi

Department of Life Sciences, Graduate School of Arts and Sciences, The University of Tokyo, Meguro-ku,
Tokyo 153, Japan

Masamichi Fujihira

Department of Biomolecular Engineering, Tokyo Institute of Technology, Nagatsuta, Midori-ku,
Yokohama 226, Japan

(Received 23 January 1995; accepted for publication 24 March 1995)

The scanning near-field optical microscopy imaging of specimens in liquid and of cultured cells in aqueous solutions is reported. A scanning near-field optical/atomic-force microscope (SNOM-AFM) was developed, in which the scanning of an optical-fiber probe cantilever over the specimen was controlled by noncontact mode AFM (dynamic mode AFM). This imaging mode reduces damage to the probe and soft specimens. The resonant frequency of the probe cantilever decreased 20% to ≈ 14 kHz and the Q factor decreased by a factor of 8 to ≈ 30 in water, compared with these values in air, which was sufficient to perform SNOM-AFM imaging in liquid. © 1995 American Institute of Physics.

Near-field optical microscopy in liquids has been long awaited for the observation of specimens in aqueous media and organic solvents with high resolution. In biology, optical microscopy is essential for studying the structural basis of functions of cells and supramolecular complexes because it allows observation of their functional states in aqueous media. However, the resolution of conventional (far-field) optical microscopy is typically several hundred nanometers, which is insufficient for observing molecular events. Electron microscopes have much better resolution, but do not allow observation in aqueous solutions.

We previously developed a new scanning near-field optical microscope (scanning near-field optical/atomic-force microscope; SNOM-AFM) in which a feedback signal from AFM in the noncontact mode was used to scan the probe tip along the surface contour of the sample.¹ An optical fiber with a sharp tip on one end was bent for use as a cantilever, and the ac amplitude of the cantilever deflection was held constant during scanning by moving the stage. If this system operates successfully in liquids, it will be good for soft samples and those with great variations in height, such as cultured cells. In this sense, for observation of biological specimens, SNOM-AFM may be superior to other systems that have been used in the atmospheric environment, such as those utilizing lateral shear force,² STM,³ and contact-mode AFM^{4,5} as a method to control sample-tip separation. In addition, an optical-fiber cantilever is round (the usual AFM cantilever is rather flat and wide), which helps to reduce viscositic resistance. Tapping mode AFM in liquids have been reported⁶ although the method of controlling the tip-sample separation is different from the present system.

In the present investigation, we further developed the SNOM-AFM system for observation of specimens in liquids.

Near-field images and AFM images (noncontact mode) were obtained simultaneously. This letter reports the observation of a standard specimen in liquid and displays near-field optical images of cultured cells in an aqueous solution. To our knowledge, near-field observation in liquid has not been reported so far.

The SNOM-AFM system is essentially the same as reported previously (Fig. 1), except that the numerical aperture of the collector lens was increased from 0.15 to 0.69 to increase the transmitted light signal, and the reflecting surface of the cantilever for laser deflection measurement was ground to replace a stainless mirror in the previous system to increase stability. The optical-fiber cantilever is mounted on a bimorph and vibrated vertically against the specimen stage at the resonant frequency (typically 10–40 kHz). Vibration amplitude is monitored by detecting the deflection of the laser beam, which is reflected on the polished surface of the glass cantilever. The probe-sample distance is controlled dynamically by decreasing the vibration amplitude as the distance between the probe and the sample decrease.

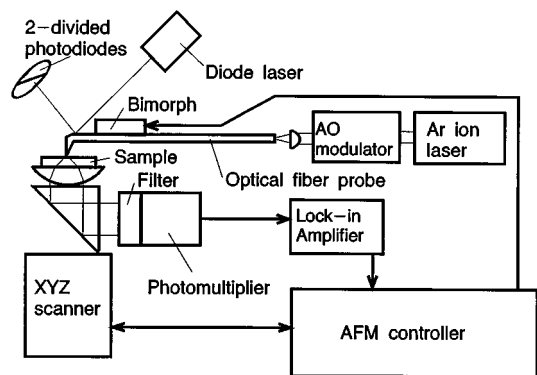


FIG. 1. Schematic diagram of the SNOM-AFM system used in the present research.

^{a)}Electronic mail: muramatu@tk.sii.co.jp

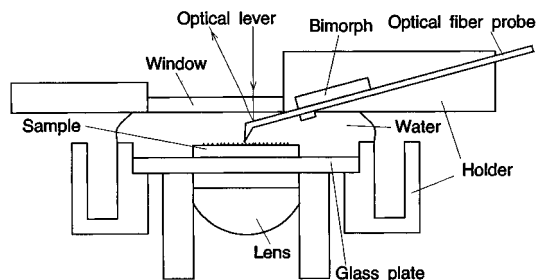


FIG. 2. Schematic diagram of the liquid cell.

Figure 2 shows a liquid cell designed for the present experiment. Water and cell culture media were held between the glass plate and an upper window. Both the probe and the sample were immersed in solution.

The probe was prepared as described previously.¹ Briefly, an optical fiber was pulled with irradiation of a CO₂ laser to make a tip, and then bent with irradiation of a CO₂ laser. The probe was coated with 200-nm-thick aluminum, and an aperture was made at the tip by chemical etching (Fig. 3).

The spring constant of the probe was 2–20 N/m as calculated on the basis of its shape (rod) and Young's modulus for quartz glass. Typically, the resonant frequency of the optical fiber tip cantilever was 17 kHz and the Q -factor was 240 in air. The resonant frequency decreased about 20% to 14 kHz and the Q -factor decreased by a factor of 8–28 when the cantilever was placed in water. This Q -factor is small, but sufficient to operate noncontact mode AFM in water.

The relationship between the vibration amplitude of the cantilever and the sample–probe distance was measured in water by varying the height of the specimen stage (Fig. 4). The ac voltage that must be applied to the bimorph to obtain a curve in water similar to that in air is greater by a factor of about 10 in water. The maximum vibration amplitude is proportional to the vibration voltage applied to the bimorph. With a decrease in the sample–probe separation, the vibration amplitude decreases as the probe approaches the sample at the extreme of each vibration cycle. The amplitude at this roll-out point is proportional to the vibration voltage between 1 and 10 ac V. The oscillation amplitude employed was between 20–200 nm (1–10 ac V for driving the bimorph). The



FIG. 3. A representative scanning electron microscope image of the probe made from an optical fiber coated with aluminum.

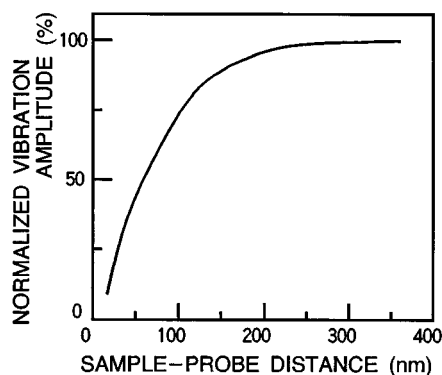


FIG. 4. Relationship between vibration amplitude of the cantilever and the sample–probe distance measured in water. A maximum vibration amplitude of 200 nm was used in this experiment, by applying 10 ac V on the bimorph.

large oscillation amplitude is due to the long cantilever, which is 2–4 nm long, while the normal cantilever probe for noncontact AFM is 200–500 μm long and shows a vibration amplitude of 10–20 nm in air.

The gradual decrease in vibration amplitude with a decrease in the sample–probe distance outside the roll-out point is characteristic of noncontact mode AFM and indicates that noncontact mode AFM operates normally in water. The steep part of the curve indicates that the cantilever is in the cyclic contact (tapping) mode. Under typical imaging conditions, average sample–probe separation was controlled so that the amplitude of the vibration became 98% of the maximum vibration (when the probe was placed far away from the sample, the range of maximum vibration amplitude employed was between 20 and 200 nm). Therefore, the interaction force between the probe and the sample is likely to be as small as that for normal tapping mode AFM.

To test the SNOM-AFM system for imaging a specimen in water, we used a 1 μm \times 1 μm checkered pattern made with 20-nm-thick chromium coating over a quartz plate. Figure 5 shows noncontact mode AFM topographic and near-field optical transmission images. In the topographic (AFM) image, the elevated areas of the chromium layer are lighter than the base (glass). The same area is darker in the near-field transmission image because the chromium coating prevents the passage of diffracted light generated due to interaction of the near-field and the chromium surface. The expanded pattern near the edge of the chromium coating (data not shown) suggests that the resolution of the present

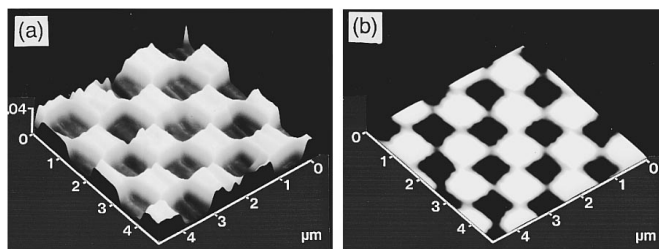


FIG. 5. Topographic (noncontact mode AFM) (a) and optical transmission (near-field transmission mode) (b) images of a 1 μm \times 1 μm checkered pattern of chromium coating over a quartz plate immersed in water obtained simultaneously.

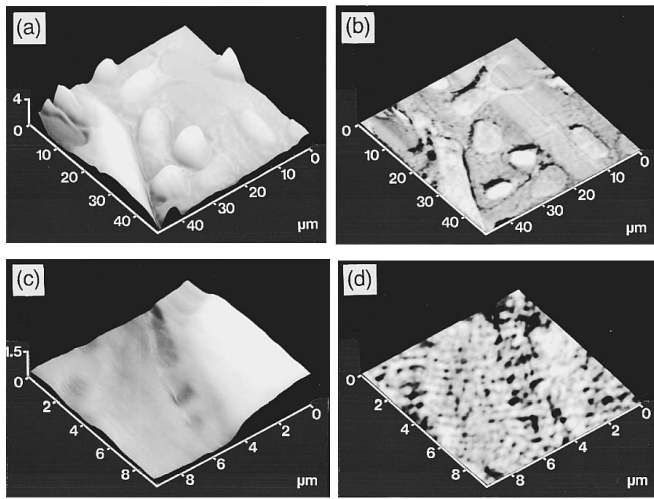


FIG. 6. Topographic (a) and (c) and near-field (b) and (d) images of cultured mouse keratinocytes in an aqueous solution. The cells were fixed by crosslinking with 2% paraformaldehyde. The areas imaged are $50\ \mu\text{m} \times 50\ \mu\text{m}$ (a) and (b) and $10\ \mu\text{m} \times 10\ \mu\text{m}$ (c) and (d).

system is better than 100 nm for aqueous samples.

Figures 6(a) and 6(b) show representative topographic and optical images of mouse keratinocyte cells in culture obtained simultaneously with the noncontact AFM mode and near-field optical transmission mode. This cell line was obtained from Dr. S. Yuspa at the National Cancer Institute, and was cultured on a $5\ \text{mm} \times 5\ \text{mm}$ cover slip as described previously.^{7,8} The cells were fixed with 2% paraformaldehyde before SNOM-AFM observation. The overall topography of the cell in lower magnification [Fig. 6(a)] is similar to that obtained for living keratinocytes as observed by contact-mode AFM in cell culture medium.⁹ The outer edges of the cells coincided in the near-field and noncontact mode AFM topographic images, while the fine structures observed in the near-field image showed no correlation with the topographic image.

Figures 6(c) and 6(d) show the images at a higher magnification. The near-field image [Fig. 6(d)] shows many filamentous structures in the cell, while the topographic image is insensitive to such structures. We examined various types of other cells, including normal rat kidney (NRK) fibroblasts, leaf cells of *boxwood*, *E.coli*, etc. The near-field images of NRK cells showed the presence of various filaments in the cell, while the latter two did not. The general feature of the

filaments of NRK cells are different from those seen in keratinocytes shown in Fig. 6(d). In some images of keratinocytes, these filaments merge with thicker filaments, which are splaying out from the near-nuclear region toward the cell borders. Similar structures were also observed in the contact-mode AFM images.

These filaments are difficult to observe in normal Nomarski and phase-contrast optical microscopy due to the lower resolution and contrast. The nature of these filaments is currently being investigated. Since they do not look like stress fibers (straight actin bundles), near-field microscopy may have selectively imaged the filaments near the apical surface of the cell.

Various filaments inside living cells can be visualized from outside the cells using the *contact mode* AFM, while topographic images of the cell by SNOM-AFM [Figs. 6(a) and 6(c)] exhibited only the surface of the cell. This result further demonstrated that the force exerted on the cell membrane is substantially weak.

Thus, SNOM-AFM introduces a new method for studying cellular structures in living cells at a resolution and contrast unobtainable by conventional optical microscopy. This technique may reveal cell characteristics until now undetected by optical microscopy of living cells or electron microscopy of processed cells. In addition, the present study suggests that the SNOM-AFM system is widely applicable to specimens in water and other fluid media.

This study was supported in part by Special Coordination Funds from the Science and Technology Agency of the Japanese government.

¹H. Muramatsu, N. Chiba, T. Ataka, H. Monobe, and M. Fujihira (unpublished).

²E. Betzig and J. K. Trautman, *Science* **257**, 189 (1992).

³U. Ch. Fischer, U. T. Dürig, and D. W. Pohl, *Appl. Phys. Lett.* **52**, 249 (1988).

⁴S. Shalom, K. Lieberman, and A. Lewis, *Rev. Sci. Instrum.* **63**, 4061 (1992).

⁵N. F. van Hulst, M. H. P. Moers, O. F. J. Noordman, R. G. Tack, F. B. Segerink, and B. Bölger, *Appl. Phys. Lett.* **62**, 461 (1993).

⁶P. K. Hansma, J. P. Cleveland, M. Radmacher, D. A. Walters, P. E. Hillner, M. Bezanilla, M. Fritz, D. Vie, and H. G. Hansma, *Appl. Phys. Lett.* **64**, 1738 (1994).

⁷M. Kulesz-Martin, A. E. Kilkeny, K. A. Holbrook, V. Digernes, and S. H. Yuspa, *Carcinogenesis (London)* **4**, 1367 (1983).

⁸A. Kusumi, Y. Sako, and M. Yamamoto, *Biophys. J.* **65**, 2021 (1993).

⁹M. Takeuchi, H. Miyamoto, H. Komizu, and A. Kusumi, *Cell Struct. Funct.* **17**, 487 (1992).